ISSN 1392 - 1207. MECHANIKA. 2008. Nr.5(73)

# Load distribution in the thread of body

**A. Krenevičius*, M. Leonavičius**, J. Selivonec*****
**Vilnius Gediminas Technical University, Saulėtekio al. 11, 10223 Vilnius, Lithuania, E-mail: kron@fm.vgtu.lt*
***Vilnius Gediminas Technical University, Saulėtekio al. 11, 10223 Vilnius, Lithuania, E-mail: minleo@fm.vgtu.lt*
****Vilnius Gediminas Technical University, Saulėtekio al. 11, 10223 Vilnius, Lithuania, E-mail: ma@fm.vgtu.lt*

## 1. Introduction

It is shown in the article [1] that the fatigue life of the internal threads of body is longer than the fatigue life of the stud/bolt threads. If the studs meet all the requirements, a separate analysis for the internal threads is not performed. If the studs do not meet the fatigue requirements for the full design life of a vessel, they can be replaced in service. The replacement or repair for a body (flange) is difficult, expensive and may be impossible. Therefore, it is important to have a reasonable estimate of load distribution in the thread of the body for using in its fatigue life prediction as a primary data.

The analogous estimation is needful for the case when a defect existing near the thread in body is forecasted. The occurrence of defects is often unavoidable in a large dimension cast iron body made by casting [2]. In this case it is essential to avoid the defect-crack growth [3-5]. At cyclic loading a tightening of a threaded connection must be chosen in suit with this requirement. Especially it is important in the case of tension body because of the favourable conditions for a defect-crack opening [6].

In analytical models of load distribution between threads the assumption that longitudinal stresses in the standard nut wall distribute evenly [7] is used. However this assumption is unusable for the stud-body connection.

The model of load distribution in the stud-body thread presented in current paper estimates the variation of longitudinal deformations in contiguous to body thread layer, which take place at receeding from turn loads locations. A stability conditions for defect-crack existance near the thread in tension body are also analized.

## 2. Basic equations for tension body

In the presented model the body *1* is a thick-walled cylinder with threaded hole (Fig. 1). Its external diameter and height are $D_{bd} > D$ and $H_{bd} \geq H + d$, where $D = 1.5d$ is external diameter of standard nut, $d$ is nominal diameter of the thread and $H$ is the length of the thread engagement in connection with stud *2*. Stud core and body are in the state of tension. Their deformations as well as deflections of the engaged turn pairs are in the elastic phase.

The representations, needed to calculate longitudinal load intensities of the turns' $q(z)$ can be obtained by using equation for the displacement compatibility of threaded connection elements. The equation for a connection with the tension body as well as with the tension nut looks as follows [7]

$$\left(\Delta_s H - \Delta_s z\right) - \left(\Delta_{bd} H - \Delta_{bd} z\right) = \delta\left(z\right) - \delta\left(H\right) \qquad (1)$$

here $\Delta_s H$ and $\Delta_s z$ variations of the stud lengths $H$ and $z$, $\Delta_{bd} H$ and $\Delta_{bd} z$ variations of the same lengths in contiguous to body thread layer, $\delta(z)$ and $\delta(H)$ deflections of the turns pairs at coordinates $z$ and $z = H$.

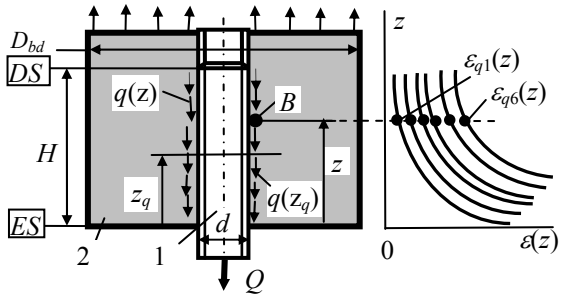


Fig. 1 Connection of stud *1* with tension body *2*

Axial force in the stud cross-section $z$ is $Q(z) = Q - \int_0^z q(z)dz$, therefore after differentiation of Eq. (1) the following differential equation was obtained

$$-\frac{Q}{E_s A_s} + \frac{1}{E_s A_s}\int_0^{z_1} q\left(z\right)dz + \varepsilon_{bd}\left(z\right) = \gamma q'\left(z\right) \qquad (2)$$

where $Q$ is external force on the stud, $E_s$ and $A_s$ are modulus of elasticity and cross-sectional area of the bolt core, $\gamma$ is pliability of the turns pair, which can be obtained experimentally [8], $\varepsilon_{bd}(z)$ is average (nominal) deformation of contiguous to the body thread layer at coordinate $z$.

Deformation $\varepsilon_{bd}(z)$ due to load intensities $q(z_q)$ (Fig. 1) depends of it's locations with respect to section $z$. For example, the deformation at point $B$ due to $q(z_{q1})$, $q(z_{q2})$...., which are located between $z = 0$ and $z$, is $\varepsilon_B = \varepsilon_{bd}(z) = \varepsilon_{q1}(z) + \varepsilon_{q2}(z) + ...$ as shown in Fig. 1 (in Fig. 2 it is shown also for the compressed body).

Deformation $\varepsilon_{bd}(z)$ of the body layer near the thread can be expressed as follows

$$\varepsilon_{bd}\left(z\right) = \int_0^z q\left(z_q\right)\varepsilon_{(1)}\left(z - z_q\right)dz_q; \quad 0 \leq z_q \leq z \qquad (3)$$

where $z_q$ is location coordinate of load intensity $q(z_q)$, $\varepsilon_{(1)}(z\text{-}z_q)$ is nominal deformation of contiguous to the body thread layer at the coordinate $z$ due to unit load intensity $q = 1$, which is located at $z_q$.

By using Eq. (3) in Eq. (2) and designating $t = 1/(E_s A_s)$ we get

$$-tQ + t\int_0^z q(z)\,dz + \int_0^z q(z_q)\,\varepsilon_{(1)}(z - z_q)\,dz_q = \gamma q'(z) \quad (4)$$

Load intensity $q(z)$, which is the solution of Eq. (4), can be expressed as series

$$q(z) = a_0 + a_1 z + a_2 z^2 + a_3 z^3 + a_4 z^4 + \ldots \quad (5)$$

where $0 \le z \le H$, and $a_0$, $a_1$, $a_2$, $a_3$, ... are factors which needs to be determined.

Function $\varepsilon_{(1)}(z\text{-}z_q)$, which is used in Eq. (4) can be also expressed as series

$$\varepsilon_{(1)}(z - z_q) = b_0 + b_1(z - z_q) + b_2(z - z_q)^2 + b_3(z - z_q)^3 \quad (6)$$

where $b_0$, $b_1$, $b_2$, $b_3$ are factors which could be determined by using *FE* technique.

Now it is useful to notice that $q(z)$ and $q(z_q)$ in Eq. 4 are the same function really. Therefore

$$q(z_q) = a_0 + a_1 z_q + a_2 z_q^2 + a_3 z_q^3 + a_4 z_q^4 + \ldots \quad (7)$$

where $0 \le z_q \le z$.

By using Eq. (6) and Eq. (7) it becomes possibly to solve integral (3)

$$\begin{aligned}
\varepsilon_{bd}(z_1) &= a_0 b_0 z_1 + \frac{1}{2}(a_1 b_0 + a_0 b_1) z_1^2 + \\
&+ \frac{1}{3}\left(a_2 b_0 + \frac{1}{2} a_1 b_1 + a_0 b_2\right) z_1^3 + \\
&+ \frac{1}{4}\left(a_3 b_0 + \frac{1}{3} a_2 b_1 + \frac{1}{3} a_1 b_2 + a_0 b_3\right) z_1^4 + \\
&+ \frac{1}{5}\left(a_4 b_0 + \frac{1}{4} a_3 b_1 + \frac{1}{6} a_2 b_2 + \frac{1}{4} a_1 b_3\right) z_1^5 + \\
&+ \frac{1}{6}\left(a_5 b_0 + \frac{1}{5} a_4 b_1 + \frac{1}{10} a_3 b_2 + \frac{1}{10} a_2 b_3\right) z_1^6 + \\
&+ \frac{1}{7}\left(a_6 b_0 + \frac{1}{6} a_5 b_1 + \frac{1}{15} a_4 b_2 + \frac{1}{30} a_3 b_3\right) z_1^7 + \\
&+ \frac{1}{8}\left(a_7 b_0 + \frac{1}{7} a_6 b_1 + \frac{1}{21} a_5 b_2 + \frac{1}{35} a_4 b_3\right) z_1^8 + \ldots\ldots
\end{aligned} \quad (8)$$

For the solution of Eq. (4) it is needful to put here integral of Eq. (5), derivative of Eq. (5) and expression (8). By comparing the factors at $z$ with the same exponents of power the factors $a_0$, $a_1$, $a_2$, $a_3$, ... have been found. After this the Eq. (5) get the next form

$$\begin{aligned}
q(z) &= a_0\left(1 + g_2 z^2 + g_3 z^3 + g_4 z^4 + \ldots\right) + \\
&+ a_1\left(z + v_3 z^3 + v_4 z^4 + v_5 z^5 + \ldots\right) = \\
&= a_0 G(z) + a_1 V(z)
\end{aligned} \quad (9)$$

where

$$\left.\begin{aligned}
&g_1 = 0, g_2 = \frac{b_0 + t}{2\gamma}, g_3 = \frac{b_1}{6\gamma} \\
&g_4 = \frac{1}{4\gamma}\left(g_2 \frac{b_0 + t}{3} + \frac{b_2}{3}\right) \\
&g_5 = \frac{1}{5\gamma}\left(g_3 \frac{b_0 + t}{4} + g_2 \frac{b_1}{12} + \frac{b_3}{4}\right) \\
&g_6 = \frac{1}{6\gamma}\left(g_4 \frac{b_0 + t}{5} + g_3 \frac{b_1}{20} + g_2 \frac{b_2}{30}\right) \\
&g_7 = \frac{1}{7\gamma}\left(g_5 \frac{b_0 + t}{6} + g_4 \frac{b_1}{30} + g_3 \frac{b_2}{60} + g_2 \frac{b_3}{60}\right) \\
&g_8 = \frac{1}{8\gamma}\left(g_6 \frac{b_0 + t}{7} + g_5 \frac{b_1}{42} + g_4 \frac{b_2}{105} + g_3 \frac{b_3}{210}\right) \\
&g_9 = \frac{1}{9\gamma}\left(g_7 \frac{b_0 + t}{8} + g_6 \frac{b_1}{56} + g_5 \frac{b_2}{168} + g_4 \frac{b_3}{280}\right) \\
&a_1 = -\frac{Qt}{\gamma}, v_1 = 1, v_3 = \frac{b_0 + t}{6\gamma}, v_4 = \frac{b_1}{24\gamma} \\
&v_5 = \frac{1}{5\gamma}\left(v_3 \frac{b_0 + t}{4} + \frac{b_2}{12}\right) \\
&v_6 = \frac{1}{6\gamma}\left(v_4 \frac{b_0 + t}{5} + v_3 \frac{b_1}{20} + \frac{b_3}{20}\right) \\
&v_7 = \frac{1}{7\gamma}\left(v_5 \frac{b_0 + t}{6} + v_4 \frac{b_1}{30} + v_3 \frac{b_2}{60}\right) \\
&v_8 = \frac{1}{8\gamma}\left(v_6 \frac{b_0 + t}{7} + v_5 \frac{b_1}{42} + v_4 \frac{b_2}{105} + v_3 \frac{b_3}{210}\right) \\
&v_9 = \frac{1}{9\gamma}\left(v_7 \frac{b_0 + t}{8} + v_6 \frac{b_1}{56} + v_5 \frac{b_2}{168} + v_4 \frac{b_3}{280}\right)
\end{aligned}\right\} \quad (10)$$

Factor $a_0$ of Eq. (9) can be defined by using boundary condition

$$Q = \int_0^H q(z)dz = a_0 \overline{G}(H) + a_1 \overline{V}(H) \quad (11)$$

here $\overline{G}(H)$ and $\overline{V}(H)$ are values of the integrals of functions $G(z)$ and $V(z)$ at $z = H$.

## 2. Basic equations for compressed body

The displacements compatibility equation for a stud connection with the compressed body as well as with the compressed nut looks as follows [7]

$$\Delta_s(z) + \Delta_{bd}(z) = \delta(z) - \delta(0) \quad (12)$$

where $\Delta_s(z)$ is variations of the stud length $z$, $\Delta_{bd}(z)$ is a variation of the same length of contiguous to the body thread layer, $\delta(z)$ and $\delta(0)$ are deflections of the turns' pairs at coordinates $z$ and $z = 0$ (Fig. 2).

As it is shown in Fig. 2 in the case of compressed body coordinate $z$ has contrary direction in comparison to the case of tension body. In this case axial force in the stud cross-section $z$ is $Q(z) = \int_0^z q(z)dz$ .

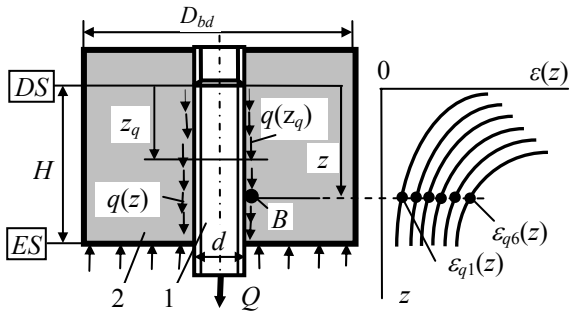


Fig. 2 Connection of stud *1* with compressed body *2*

Distribution of load intensities in the thread has been obtained in the same way as in the case of the tension body. The solutions for compressed body get the forms of Eq. (8-11), in which factor $a_1 = 0$.

### 3. Nominal longitudinal strains in the body layer near the threads at unit load intensity $q = 1$

In the cases of stud-nut connections for the solution of Eq. (1) or Eq. (12) the nominal (average) longitudinal strains of the stud core and nut wall are used. In the case of the body the concept of nominal elastic strains is fitted only to longitudinal layer near the internal thread and is expressed by Eq. (3). At unit load intensity $q_{(1)}$=1 it is set in Eq. (6). The factors of Eq. (6) have been found by using derivative of Eq. (13), which expresses longitudinal displacements $\Delta_{(1)}(z - z_q)$ in the body layer near the thread *m* - *n* (Fig. 3) due to unit load intensity $q_{(1)}$=1 kN/mm

$$\Delta_{(1)}\left(z-z_q\right) = \int_{z_q}^{z} \varepsilon_{(1)}\left(z-z_q\right)dz = e_1\left(z-z_q\right) + \\ + e_2\left(z-z_q\right)^2 + e_3\left(z-z_q\right)^3 + e_4\left(z-z_q\right)^4 \qquad (13)$$

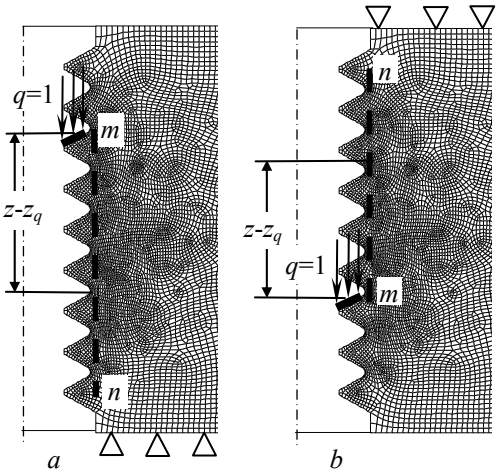


Fig. 3 Finite element mesh of the threaded body: a - compressed body; b - tension body line *m*-*n* is layer near the threads

The factors of Eq. (13) have been found by using data of FE analysis (Fig. 3) and least-squares technique. So the factors of Eq. (6) are $b_0 = e_1$, $b_1 = 2e_2$, $b_2 = 3e_3$, $b_3 = 4e_4$.

The FE analysis was carried out using the ANSYS version 10.0 suite of programs. The body with circular turns was modelled using two-dimensional isoparametric elements with eight nodes of two degrees of freedom at each node. Axisymmetric type of analysis was carried out using only half of a section in length. FE mesh (Fig. 3) was unstructured, it consist of PLANE 183 elements. The geometry of the body threads based on ISO M20×2.5 was modeled. Material of the body is cast iron (modulus of elasticity $E = 160$ GPa and Poisson's ratio $\nu = 0.26$).

Longitudinal displacements in tension body layer near the thread obtained by FE analysis (points) and by least-squares technique (lines) are shown in Fig. 4.

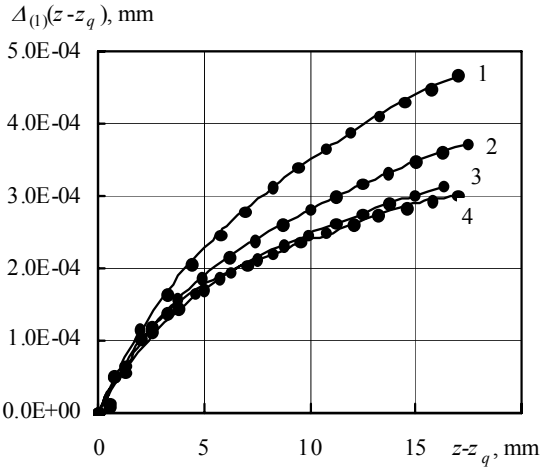


Fig. 4 Longitudinal displacements in tension body at $q$ = 1.0 kN/mm: *1* - $D_{bd}$ = 30 mm, *2* - 40 mm, *3* - 60 mm, *4* - 80 mm

The values of the factors of Eq. (6) for cast iron bodies with internal thread M20×2.5 are presented in Table.

Table

The values of the factors of Eq. (6) for cast iron bodies

| $D_{bd}$ mm | $b_0$ | $b_1$ | $b_2$ | $b_3$ |
|---|---|---|---|---|
| M20×2.5; $E$=160GPa; ν =0.26; compressed body | | | | |
| 30 | 6.87E-05 | -8.5E-06 | 3.736E-07 | -3.9E-9 |
| 40 | 4.61E-05 | -8.09E-06 | 4.88E-07 | -1.02E-8 |
| 60 | 4.01E-05 | -7.53E-06 | 4.78E-07 | -9.62E-9 |
| 80 | 3.84E-05 | -6.46E-06 | 4.15E-07 | -8.88E-9 |
| M20×2.5; $E$=160GPa; ν =0.26; tension body | | | | |
| 30 | 6.63E-05 | -1.11E-05 | 9.33E-07 | -2.82E-8 |
| 40 | 5.68E-05 | -9.88E-06 | 7.87E-07 | -2.20E-8 |
| 60 | 5.20E-05 | -9.27E-06 | 7.15E-07 | -1.90E-8 |
| 80 | 5.99E-05 | -1.29E-05 | 1.06E-06 | -2.85E-8 |

### 4. Distribution of load between turns and deformations of the layer near the thread in the body

By above stated technique the load distribution in the thread and deformation of the body has been calculated for connections ISO M20x2.5 which lengths are $H$=16 mm (Figs. 5-7). Steel 4130 was used for the stud and cast iron SG was used for the tension body. Average indices of mechanical properties of steel 4130: $R_{pr} = 621$ MPa, $R_{p0.2} = 766$ MPa, $R_m = 930$ MPa, $Z = 59$ %, $E_s = 185$ GPa. Average indices of mechanical properties of body material

cast iron SG: $R_{p0.2} = 615$ MPa, $R_m = 870$ MPa, $Z = 3.0$ %, $E_{bd} = 160$ GPa. Experimentally obtained pliability of the turns pair by using special connection M20x2.5 is $\gamma = 5.26 \cdot 10^{-6}$ m/(MN/m). For this the stud with a single turn and threaded body were made from steel 4130 and cast iron SG respectively.

Calculations of the load distribution in the thread have been performed at $\sigma_{sn}/R_{p0.2} = 0.23$ where $\sigma_{sn}$ is nominal stresses of stud.

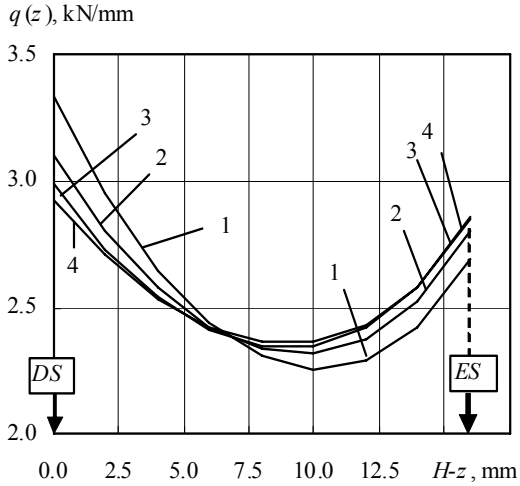


Fig. 5 Load distribution in the thread of tension body: *1* - $D_{bd}$ = 30 mm, *2* - 40 mm, *3* - 60 mm, *4* - 80 mm

In the case of tension bodies the values of load intensities $q_{bd}(H)$ and of longitudinal strains near the internal thread $\varepsilon_{bd}(H)$ are the highest at depth $H$ (in the deepest section *DS* according Fig. 1) as shown in Fig. 5 and Fig. 6. The values $q_{bd}(H)$ obtained for the tension bodies $D_{bd}$ = 40, 60, 80 mm are by 6.8%, 10.3% and 12.1% less respectively than that obtained for detail $D_{bd}$ = 30 mm.

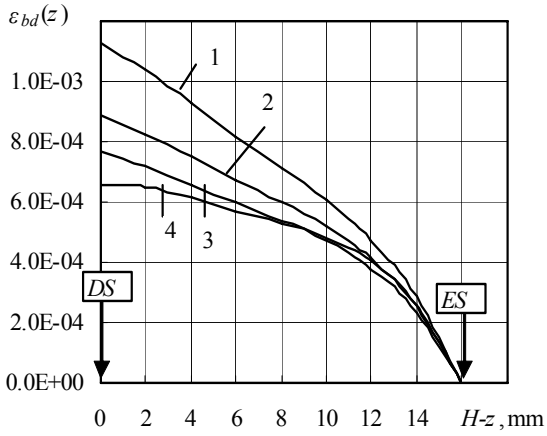


Fig. 6 Deformation in tension body layer near the thread: *1* - $D_{bd}$=30 mm, *2* - 40 mm, *3* - 60 mm, *4* - 80 mm

The values of $\varepsilon_{bd}(H)$ are by 21.1, 31.7 and 41.5% less at comparison in the same order.

It is necessary to notice here that wall thickness of the external detail with $D_{bd}$ = 30 mm is the same as of the standard nut. In this case because of least wall thickness the value of strain $\varepsilon_{bd}(H)$ is the highest.

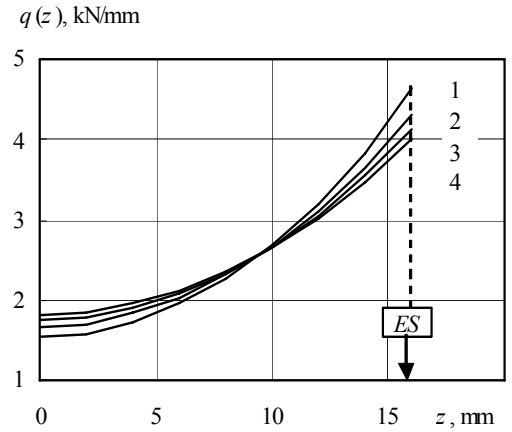


Fig. 7 Load distribution in the thread of compressed body: *1*, *2*, *3*, *4* - $D_{bd}$ = 30, 40, 60, 80 mm

In the case of compressed bodies the values of load intensities $q_{bd}(H)$ are the highest in the entry section *ES* (Fig. 7). The location of *ES* is shown in Fig. 2. The values $q_{bd}(H)$ obtained for the compressed bodies $D_{bd}$ = 40, 60, 80 mm are by 6.9%, 10.6% and 13.7% less respectively than that obtained for the nut (detail $D_{bd}$ = 30 mm).

## 5. Determination of tightening stresses for threaded body with defect

Often structural bodies of large dimensions are manufactured by using cast iron mouldings in which various defects and voids are met. Sometimes modeling of the bodies assumes that small void is situated near the thread of threaded hole. This void is identified like a crack. In cast iron SG which is used in mining industry equipment, typical dimension of voids is 1-4 mm (Fig. 8).

The study presented in the previous sections may be useful for a preliminary consideration of tightening conditions in the case of tension body with defect near the internal thread. A defined level of tightening should safeguard against void-crack increasing. A void-crack may slightly increase at high cyclic loading if it stick at the root of internal thread. However increasing of the crack must be stopped when the crack tip leaves a zone of stress concentration. Analysis of the fatigue failure surfaces of the studs shows this zone deep to be about 0.36*P*, where *P* is thread pitch. This dimension was used for the threaded bodies too.

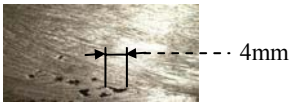


Fig. 8 The voids in cast iron SG

Preliminary tightening stresses have been defined for threaded connection M20x2.5. The dimensions of schematic tension body were $D_{bd}$ = 60 mm, $H$ = 16 mm and the wall thickness $h$ = 20 mm. Mechanical properties of used connection elements were the same like given in section 4.

The nominal stresses in the stud after tightening is $\sigma_{s,t} = Q/A_s$. The average stresses of the body layer $m$ - $n$ (Fig. 3) here is called nominal body stresses, which are as follows

$$\sigma_{bd,t}(z) = \varepsilon_{bd}(z) E_{bd} \tag{14}$$

The highest stress $\sigma_{bd,t}(H)$ appeared in the body's deepest section *DS* (Fig. 1). Relation of the stresses $\sigma_{s,t}$ and $\sigma_{bd,t}(H)$ may be defined by using the calculating method given in the section 2. It was assumed that void-crack has semielliptical form, which depth is $c$>0.36$P$ and length 3$c$ (Fig. 9). Crack is situated at the free internal threaded surface in the deepest section *DS*.

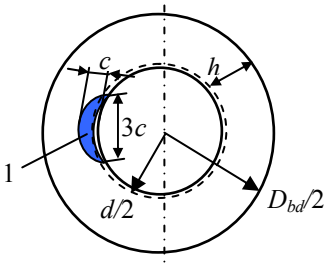


Fig. 9 Crack *1* in the tension body cross-section *DS*

According to linear fracture mechanics in case of elastic cyclic loading the condition of the body crack stability can be as follows

$$\Delta K \le \Delta K_{th,r} / n_s \tag{15}$$

where $\Delta K$ is stress intensity factor range for the body crack, to be precise $\Delta K = K_{1,max} - K_{1,min}$, where $K_{1,max}$ and $K_{1,min}$ are maximum and minimum values of the stress intensity factor in loading cycle; $\Delta K_{th,r}$ is crack threshold for the body material at asymmetry cyclic loading; $r$ is asymmetry factor of the loading cycle, to be precise $r = K_{1,min} / K_{1,max}$; $n_s$ is safety factor.

Unfortunately, in the text books [9-11] and other literature on fracture mechanics authors do not meet with success to find formulae for the calculation of $K_1$ (stress intensity factor for mode 1) in the case of internal semi-elliptical crack which is situated in the thick-walled cylinder (Fig. 9). Therefore, after special correction the formulae for calculating of the stress intensity factor $K_1^{circl}$ in the case of circular internal crack, which is situated in the thick-walled cylinder (Fig. 10), was used [10]

$$K_1^{circl} = \sigma \sqrt{\pi c} F_1 \tag{16}$$

where $F_1$ is the function dependent on ratio $T = c/h$.

By using the data given in Tables of the article [10], function $F_1$ have been expressed by cubic equation: $F_1 = 1.0867 - 1.0322T + 1.6409T^2 + 0.2685T^3$.

To ascertain the magnitude of the correction coefficient for using of formulae (16) in case shown in Fig. 9 the two values of stress intensity factors ($K_1^*$ and $K_1^{**}$) have been compared. Its have been calculated for semi-elliptical and circular cracks situated in two plates as are shown in Fig. 11, a and b by using the formulas given in the article [9].

These cracks had the same depth $c$ and analogous forms to those which are shown in Fig. 9 and Fig. 10 respectively. Also the plates and the considered cylinder body had the same thickness $h$ = 20 mm.

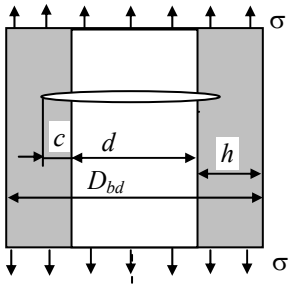


Fig. 10 Thick-walled cylinder with circular crack

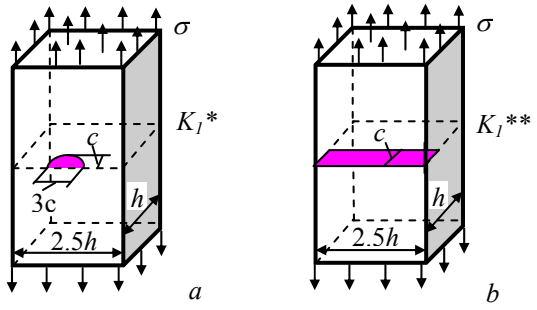


Fig. 11 Cracked plates: a - with semielliptical crack b - cracked over all width

The calculated values of ratio $K_1$*/ $K_1$** are 1.42, 1.47, 1.55, 1.65 and 1.74 at crack depths $c$ = 1, 2, 3, 4, 5 mm respectively.

The same analysis was performed for two pipes too. The crack in the first pipe had semi-elliptical form like as in Fig. 9. In the second pipe the crack was circular like as in Fig. 10. Dimensions of pipes were $d$ = 20 mm and $h$ = 2 mm. The values of stress intensity factors $\overline{K}_1^*$ and $\overline{K}_1^{**}$ for the first and the second pipes have been calculated by using the formulas given in the article [11]. The obtained values of the ratio $\overline{K}_1^* / \overline{K}_1^{**}$ are 1.4 and 1.77 at crack depths $c$ = 0.5 mm and $c$ = 1.0 mm respectively.

It can be noticed that in both cases of the performed comparisons considered ratio is more than 1.4. For preliminary analysis the same can be assumed for the case of thick-walled cylinder too. So, the stress intensity factor for the internal semi-elliptical crack in the thick-walled cylinder have been calculated by using formulae (16) with the correction coefficient

$$K_1 = \frac{K_1^{circl}}{1.4} \tag{17}$$

By using formula (17) and (16), in which $\sigma$ = = $\sigma_{bd,t}(H)$, relation between $K_1$ and nominal tightening stresses $\sigma_{bd,t}(H)$ and $\sigma_{s,t}$ for the case of tension body (M20 x 2.5, $D_{bd}$ = 60mm) with internal semi-elliptical crack (Fig. 12) have been found.

To settle tightening parameters for the considered threaded connection the condition (15) should be met. For this the allowable mean stress intensity factor $K_m$ in the loading cycle must be defined because it meets the state of crack after the connection tightening. By using allowable value of $K_m$ the allowable tightening stresses $\sigma_{s,t}$ and $\sigma_{bd,t}(H)$ could be determined from the graphs in Fig. 12.

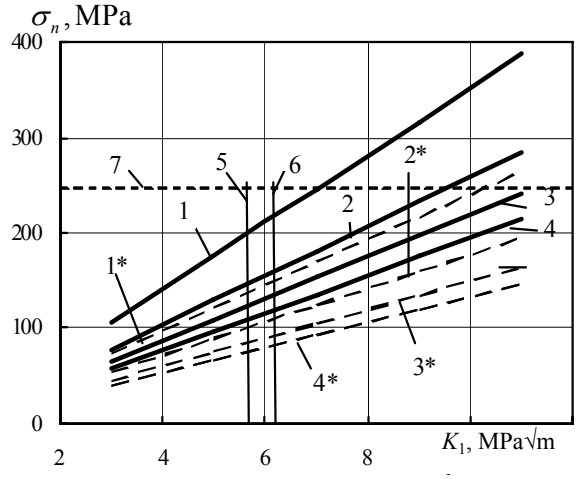


Fig. 12 Stress intensity factor dependencies on tightening of threaded connection: *1*, *2*, *3*, *4* - $\sigma_n = \sigma_{s,t}$; *1**, *2**, *3**, *4** - $\sigma_n = \sigma_{bd,t}(H)$; crack depth *c*: *1*, *1**- 1 mm; *2*, *2**- 2 mm; *3*, *3**- 3 mm; *4*, *4**- 4 mm; *5* and *6* - $K_m$ = 5.7 and 6.1 MPa$\sqrt{\text{m}}$, *7* - $\sigma_{s,t} = 0.4R_{pr}$

The mean stress intensity factor is

$$K_m = K_{max} - \frac{\Delta K}{2} = \Delta K \frac{1+r}{2(1-r)} \qquad (18)$$

because $K_{max} = \Delta K / (1-r)$.

To avoid the crack growth it is necessary in formulae (18) to use $\Delta K = \Delta K_{th,r}/n_s$, where $n_s$ is safety factor.

In the example under consideration the body is made from cast iron SG which is used for mining equipment manufacturing. For determining the threshold $\Delta K_{th,0}$ (at $r = 0$) five compact tension CT specimens (M1 - M5) were tested in accordance with the ASTM E 647-00 methods. Thickness and width of the specimens were $B$ = 25mm and $W$ = 50mm. The obtained crack growth rate versus stress intensity factor range fatigue diagram is shown in Fig. 13. The average value of threshold $\Delta K_{th,0}$ is 9.5 MPa$\sqrt{\text{m}}$.

The value of threshold $\Delta K_{th,r}$ at $r > 0$ may be found by using expression [10]

$$\Delta K_{th,r} = \Delta K_{th,0} (1-r)^{\lambda} \qquad (19)$$

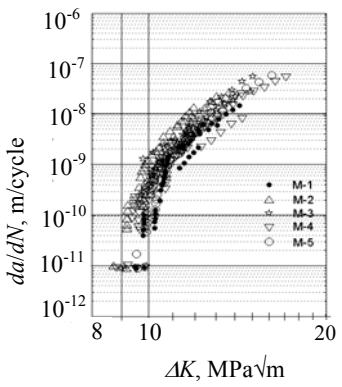


Fig. 13 Fatigue crack growth

where exponent of power $\lambda$ = (0.5-1) for steels and $\lambda$ = 1 for cast irons.

In the final analysis the allowable tightening stresses of the stud can be defined approximately for the case of tension body (M20 x 2.5, $D_{bd}$ = 60 mm) with the internal semielliptical crack (Fig. 9).

The asymmetry factor at high cyclic loading for mining equipment usually is in range $r$ = 0.7-0.95 and the safety factor can be $n_s$ = 1.5. By using formulae (18) and (19) it was obtained: $K_m$ = 5.4 MPa$\sqrt{\text{m}}$, when $r$ = 0.7 and $K_m$ = 6.2 MPa$\sqrt{\text{m}}$, when $r$ = 0.95. These values of $K_m$ are marked in Fig. 12 by the vertical lines *5* and *6*. It can be seen in Fig. 12 that tightening stresses $\sigma_{s,t}$ of the stud at various crack depths *c* (lines *1*, *2*, *3*, *4*) are disposed below the horizontal line *7*, which reflect $\sigma_{s,t} = 0.4R_{pr}$, and between lines *5* and *6*. It shows the tightening stresses of the stud are less than $\sigma_{s,t} = (0.4\text{-}0.6)R_{pr}$, which is recommended to safeguard stability of tight [7].

So, at setting conditions for crack stability in the case of threaded tension body the problem of connection release arises, which should be analysed in particular.

In design stage it would be useful to change the construction of connected parts in order to get a compressed condition in the threaded body. Then the possibility of crack growth in the body would be considerably less and the tight could be bigger.

**6. Conclusions**

1. The proposed model of the load distribution in the thread of stud-body connection estimates the variation of longitudinal strains in contiguous to the body thread layer, which take place at the receeding from the location of the turn loads.

2. The increasing of the body volume around the internal thread (increasing of $D_{bd}$) the maximum value of the turn load intensity in stud-body connection thread decreases.

3. In the case of tension bodies the values of turn load intensities $q_{bd}(H)$ and the values of longitudinal strains near the internal thread $\varepsilon_{bd}(H)$ are the highest in the deepest cross-section of bodies *DS* where the turns engagement take place. In the case of compressed bodies the same is obtained in the opposing cross-section *ES* of the bodies.

4. The highest values of the turn load intensities $q_{bd}(H)$ in threads of examined cast iron compressed bodies $D_{bd}$=40, 60, 80 mm are respectively less by 6.9, 10.6 and 13.7% than that obtained for the nut (detail $D_{bd}$=30 mm) and the like it is in the cases of tension bodies. In these cases the values of the longitudinal strains near the internal thread $\varepsilon_{bd}(H)$ are by 21.1, 31.7 and 41.5% less in comparison with the same order as above.

5. In accordance with the preliminary calculation the problem of connection release arises if the condition for crack stability has been applied and when the crack is situated in the cast iron threaded tension body near the thread and connection experience the high cyclic loading.

**References**

1. **Kumar, R.** Fatigue life estimation for internal threads in class 1 components.-J. of Pressure Vessel Technology, ASME, 1998, v.120, p.81-85.
2. **Goodrich, G.** Cast Iron Microstructure Anomalies and Their Cause. AFS Transactions. -Illinois, Inc., Des Plaines, American Foundry Society, 1997.-669p.
3. **Taraškevičius, A., Daunys M., Narvydas E.** Experimental and numerical investigation of crack surface opening under cyclic loading. -Mechanika. -Kaunas: Technologija, 2002, Nr.3(35), p.5-10.
4. **Zdenek K.** Fuzzy probability analysis of the fatigue resistance of steel structural members under bending. -J. of Civil Engineering and Management. -Vilnius: Technika, 2008, No14(1), p.67-72.
5. **Tretjekovas, J., Kačianauskas, R., Šimkevičius, Č.** FE simulation of rupture of diapragm with initiated defect. -Mechanika. -Kaunas: Technologija, 2006, Nr.6(62), p.5-11.
6. **Medekšas, H., Balina, V.** Some aspects of lifetime modeling of power equipment elements. -Mechanika. -Kaunas: Technologija, 2002, Nr.1(33), p.17-21.
7. **Birger, I.A., Iosilevich, G.B.** Bolt and Flange Connections. -Moscow: Mashinostroenije, 1990.-365p. (in Russian).
8. **Speičys, A., Krenevičius, A.** Load distribution between threads at elastic-plastic deformations. -Mashinovedenije. -Moscow: Nauka, 1987, No2, p.87-92 (in Russian).
9. **Murakami, Y.** Stress Intensity Factors Handbook. -Moscow: Mir, 1990, v. 1 and 2.-1013p. (in Russian).
10. **Panasiuk, V., Savruk, M.** Fracture Mechanics and Strength of Materials. -Kiev: Naukova Dumka, 1988-1990, v.1.-488p., v.2.-620p., v.4.-680p.
11. **Anderson, T.** Fracture Mechanics. -Boston: CRC Press, 2005.-622p.

A. Krenevičius, M. Leonavičius, J. Selivonec

APKROVOS PASISKIRSTYMAS KORPUSO SRIEGYJE

R e z i u m ė

Straipsnyje pateiktas apkrovos pasiskirstymo korpuso sriegyje analitinis modelis, įvertinantis išilginių deformacijų kitimą, pasireiškiantį korpuso sriegiui gretimame sluoksnyje tolstant nuo vijų apkrovų pridėties vietos. Korpuso sienelės storio įtaka šiam kitimui, veikiant vienetiniam jėgos intensyvumui, nustatyta BE metodu. Apskaičiuotas apkrovos pasiskirstymas plieninės smeigės jungčių su gniuždomu ir tempiamu korpusais, pagamintais iš ketaus, sriegio vijose.

Straipsnyje pateiktas sudaryto modelio taikymo pavyzdys, kuriame preliminariai analizuojamas defekto, esančio šalia sriegio tempiamame ketaus korpuse, stabilumo ir jungties įveržimo ryšys, veikiant daugiaciklei apkrovai.

A. Krenevičius, M. Leonavičius, J. Selivonec

LOAD DISTRIBUTION IN THE THREAD OF BODY

S u m m a r y

This paper presents the analytical model of load distribution in the body thread. The model estimates a variation of longitudinal strains in contiguous to the body thread layer, which takes place at the receeding from the locations of the turn loads. The influence of the wall thickness of the cast iron body in case of this variation at unit force is assessed by FE method. Load distributions on the turns are calculated for the steel stud connections with the compressed and tension bodies of cast iron.

This paper also presents the application of the proposed model to a preliminary analysis of the relation between the stability condition of the internal defect of the tension body and the tight of the connection at high cyclic loading.

A. Кренявичюс, М. Ляонавичюс, Е. Селивонец

РАСПРЕДЕЛЕНИЕ НАГРУЗКИ ПО ВИТКАМ РЕЗЬБЫ В КОРПУСЕ

Р е з ю м е

В настоящей работе предложена аналитическая модель распределения нагрузок по виткам резьбы в корпусе. Модель учитывает изменение продольных деформаций в соседнем к резьбе слое корпуса при удалении от места приложения нагрузок на витках. Влияние толщины чугунного корпуса на такое изменение при единичном усилии на витке определено методом конечных элементов.

Приведен пример использования модели для приближенного анализа связи между условием стабильности дефекта находящегося вблизи к резьбе растягиваемого корпуса с напряжениями затяга в шпильке при многоцикловом нагружении соединения.

Received August 12, 2008

DOI: 10.5755/j02.mech.15158